

Poisson's ratio in cubic materials

By Andrew N. Norris*

Mechanical and Aerospace Engineering, Rutgers University, Piscataway, NJ 08854-8058, USA

Expressions are given for the maximum and minimum values of Poisson's ratio ν for materials with cubic symmetry. Values less than -1 occur if and only if the maximum shear modulus is associated with the cube axis and is at least 25 times the value of the minimum shear modulus. Large values of $|\nu|$ occur in directions at which the Young modulus is approximately equal to one half of its 111 value. Such directions, by their nature, are very close to 111. Application to data for cubic crystals indicates that certain Indium Thallium alloys simultaneously exhibit Poisson's ratio less than -1 and greater than +2.

Keywords: Poisson's ratio; cubic symmetry; anisotropy

1. Introduction

The Poisson's ratio ν is an important physical quantity in the mechanics of solids, arguably second only in significance to the Young modulus. It is strictly bounded between -1 and 1/2 in isotropic solids, but no such simple bounds exist for anisotropic solids, even for those closest to isotropy in material symmetry: cubic materials. In fact, Ting & Chen (2005) demonstrated that arbitrarily large positive and negative values of Poisson's ratio could occur in solids with cubic material symmetry. The key requirement is that the Young modulus in the 111direction is very large (relative to other directions), and as a consequence the Poisson's ratio for stretch close to but not coincident with the 111-direction can be large, positive or negative. Ting & Chen's result replaces conventional wisdom (e.g. Baughman et al. 1998) that the extreme values of ν are associated with stretch along the face diagonal (110-direction). Boulanger & Hayes (1998) showed that arbitrarily large values of $|\nu|$ are possible in materials of orthorhombic symmetry. Both pairs of authors analytically constructed sets of elastic moduli, which show the unusual properties while still physically admissible. The dependence of the large values of Poisson's ratio on elastic moduli and the related scalings of strain are discussed by Ting (2004) for cubic and more anisotropic materials.

To date there is no anisotropic elastic symmetry for which there are analytic expressions of the extreme values of Poisson's ratio for all materials in the symmetry class, although bounds may be obtained for some specific pairs of directions for certain material symmetries. For instance, Lempriere (1968)

^{*}norris@rutgers.edu

considered Poisson's ratios for stretch and transverse strain along the principal directions, and showed that it is bounded by the square root of the ratio of principal Young's moduli, $|\nu(n,m)| < (E(n)/E(m))^{1/2}$ (in the notation defined below). Gunton & Saunders (1975) performed some numerical searches for the extreme values of ν in materials of cubic symmetry. However, the larger question of what limits on ν exist for all possible pairs of directions remains open, in general. This paper provides an answer for materials of cubic symmetry. Explicit formulae are obtained for the minimum and maximum values of ν which allow us to examine the occurrence of the unusually large values of Poisson's ratio and the conditions under which they appear. Conversely, we can also define the range of material parameters for which the extreme values are of 'standard' form, i.e. associated with principal pairs of directions such as $\nu(110,1\bar{1}0)$ for stretch and measurement along the two face diagonals. For instance, we will see that a necessary condition that one or more of the extreme values of Poisson's ratio is not associated with a principal direction is that $\nu(110,1\overline{10})$ must be less than -1/2. The general results are also illustrated by application to a wide variety of cubic materials, and it will be shown that values of $\nu < -1$ and $\nu > 2$ are possible for certain stretch directions in existing solids.

We begin in §2 with definitions of moduli and some preliminary results. An important identity is presented which enables us to obtain the extreme values of both the shear modulus and Poisson's ratio for a given choice of the extensional direction. Section 3 considers the central problem of obtaining extreme values of ν for all possible pairs of orthogonal directions. The solution requires several new quantities, such as the values of ν associated with principal direction pairs. Section 4 describes the range of possible elastic parameters consistent with positive definite strain energy. The explicit formulae, the global extrema, are presented and their overall properties are discussed in §5. It is shown that certain Indium Thallium alloys simultaneously display values of ν below -1 and above +2.

2. Definitions and preliminary results

The fourth order tensors of compliance and stiffness for a cubic material, **S** and $C = S^{-1}$, may be written (Walpole 1984) in terms of three moduli κ , μ_1 and μ_2 ,

$$\mathbf{S}^{\pm 1} = (3\kappa)^{\mp 1} \mathbf{J} + (2\mu_1)^{\mp 1} (\mathbf{I} - \mathbf{D}) + (2\mu_2)^{\mp 1} (\mathbf{D} - \mathbf{J}). \tag{2.1}$$

Here, $I_{ijkl}=(1/2)(\delta_{ik}\delta_{jl}+\delta_{il}\delta_{jk})$ is the fourth order identity, $J_{ijkl}=(1/3)\delta_{ij}\delta_{kl}$, and

$$D_{ijkl} = \delta_{i1}\delta_{i1}\delta_{k1}\delta_{l1} + \delta_{i2}\delta_{i2}\delta_{k2}\delta_{l2} + \delta_{i3}\delta_{i3}\delta_{k3}\delta_{l3}. \tag{2.2}$$

The isotropic tensor J and the tensors of cubic symmetry (I-D) and (D-J) are positive definite (Walpole 1984), so the requirement of positive strain energy is that κ , μ_1 and μ_2 are positive. These three parameters, called the 'principal elasticities' by Kelvin (Thomson 1856), can be related to the standard Voigt stiffness notation: $\kappa = (c_{11} + 2c_{12})/3$, $\mu_1 = c_{44}$ and $\mu_2 = (c_{11} - c_{12})/2$. Alternatively, $\kappa = (s_{11} + 2s_{12})^{-1}/3$, $\mu_1 = s_{44}^{-1}$ and $\mu_2 = (s_{11} - s_{12})^{-1}/2$ in terms of the compliance.

Vectors, which are usually unit vectors, are denoted by lowercase boldface, e.g. n. The triad $\{n, m, t\}$ represents an arbitrary orthonormal set of vectors.

Directions are also described using crystallographic notation, e.g. $n = 1\bar{1}0$ is the unit vector $(1/\sqrt{2}, -1/\sqrt{2}, 0)$. The summation convention on repeated indices is assumed.

(a) Engineering moduli

The Young modulus $E(\mathbf{n})$ sometimes written $E_{\mathbf{n}}$, shear modulus $G(\mathbf{n}, \mathbf{m})$ and Poisson's ratio $v(\mathbf{n}, \mathbf{m})$ are (Hayes 1972)

$$E(\mathbf{n}) = 1/s'_{11}, \quad G(\mathbf{n}, \mathbf{m}) = 1/s'_{44}, \quad \nu(\mathbf{n}, \mathbf{m}) = -s'_{12}/s'_{11},$$
 (2.3)

where $s'_{11} = s_{ijkl} n_i n_j n_k n_l$, $s'_{12} = s_{ijkl} n_i n_j m_k m_l$ and $s'_{44} = 4 s_{ijkl} n_i m_j n_k m_l$. Thus, $E(\boldsymbol{n})$ and $\nu(\boldsymbol{n}, \boldsymbol{m})$ are defined by the axial and orthogonal strains in the \boldsymbol{n} - and \boldsymbol{m} -directions, respectively, for a uniaxial stress in the \boldsymbol{n} -direction. E and G are positive, while ν can be of either sign or zero. A material for which $\nu < 0$ is called auxetic, a term apparently introduced by K. Evans in 1991. Gunton & Saunders (1975) provide an earlier informative historical perspective on Poisson's ratio. Love (1944) reported a Poisson's ratio of 'nearly -1/7' in Pyrite, a cubic crystalline material.

The tensors I and J are isotropic, and consequently the directional dependence of the engineering quantities is through D. Thus,

$$\frac{1}{E} = \frac{1}{9\kappa} + \frac{1}{3\mu_2} - \left(\frac{1}{\mu_2} - \frac{1}{\mu_1}\right) F(\mathbf{n}),\tag{2.4}$$

$$\frac{1}{G} = \frac{1}{\mu_1} + \left(\frac{1}{\mu_2} - \frac{1}{\mu_1}\right) 2D(\boldsymbol{n}, \boldsymbol{m}), \tag{2.5}$$

$$\frac{\nu}{E} = -\frac{1}{9\kappa} + \frac{1}{6\mu_2} - \left(\frac{1}{\mu_2} - \frac{1}{\mu_1}\right) \frac{1}{2} D(\boldsymbol{n}, \boldsymbol{m}), \tag{2.6}$$

where

$$F(\mathbf{n}) = n_1^2 n_2^2 + n_2^2 n_3^2 + n_3^2 n_1^2, \quad D(\mathbf{n}, \mathbf{m}) = n_1^2 m_1^2 + n_2^2 m_2^2 + n_3^2 m_3^2. \tag{2.7}$$

We note for future reference the relations

$$D(\boldsymbol{n}, \boldsymbol{m}) + D(\boldsymbol{n}, \boldsymbol{t}) = 2F(\boldsymbol{n}). \tag{2.8}$$

(b) General properties of E, G and related moduli

Although interested primarily in the Poisson's ratio, we first discuss some general results for E, G and related quantities in cubic materials: the area modulus A, and the traction-associated bulk modulus K, defined below. The extreme values of E and G follow from the fact that $0 \le F \le 1/3$ and $0 \le D \le 1/2$ (Walpole 1986; Hayes & Shuvalov 1998). Thus, $G_{\min, \max} = \min$, $\max(\mu_1, \mu_2)$, $E_{\min, \max} = 3[(3\kappa)^{-1} + G_{\min, \max}^{-1}]^{-1}$ and E_{\min} , $E_{\max} = E_{001}$, E_{111} for $\mu_1 > \mu_2$, with the values reversed for $\mu_1 < \mu_2$ (Hayes & Shuvalov 1998). As noted by Hayes & Shuvalov (1998), the difference in extreme values of E and G are related by

$$3/E_{\min} - 3/E_{\max} = 1/G_{\min} - 1/G_{\max}.$$
 (2.9)

The extreme values also satisfy

$$3/E_{\min, \max} - 1/G_{\min, \max} = 1/(3\kappa).$$
 (2.10)

The shear modulus G achieves both minimum and maximum values if n is directed along face diagonals, that is, $G_{\min} \leq G \leq G_{\max}$ for n = 110. The area modulus of elasticity A(n) for the plane orthogonal to n is the ratio of

The area modulus of elasticity A(n) for the plane orthogonal to n is the ratio of an equibiaxial stress to the relative area change in the plane in which the stress acts (Scott 2000). Thus, $1/A(n) = s_{ijkl}(\delta_{ij} - n_i n_j)(\delta_{kl} - n_k n_l)$. Using the equations above it may be shown that, for a cubic material,

$$1/A(n) - 1/E(n) = 1/(3\kappa). \tag{2.11}$$

The averaged Poisson's ratio $\bar{\nu}(n)$ is defined as the average over m in the orthogonal plane, or $\bar{\nu}(n) = [\nu(n, m) + \nu(n, t)]/2$. The following result, apparently first obtained by Sirotin & Shaskol'skaya (1982), follows from the relations (2.8),

$$[1 - 2\bar{\nu}(\mathbf{n})]/E(\mathbf{n}) = 1/(3\kappa). \tag{2.12}$$

Equation (2.12) indicates that the extrema of $\bar{\nu}(n)$ and E(n) coincide. The traction-associated bulk modulus K(n), introduced by He (2004), relates the uniaxial stress in the n-direction to the relative change in volume in anisotropic materials. It is defined by $3K(n) = 1/s_{iikl}n_kn_l$, and for cubic materials is simply $K(n) = \kappa$. It is interesting to note that the relations (2.10)–(2.12) have the same form as for isotropic materials, for which E, G, ν , A and K are constants. Equations (2.4)–(2.6) imply other identities, e.g. that the combination $1/G + 4\nu/E$ is constant.

Further discussion of the extremal properties of G and ν requires knowledge of how they vary with m for given n, and in particular, the extreme values as a function of m for arbitrary n, considered in $\S 2c$. Note that, n = 111 and n = 001 are the only directions for which $\nu(n, m)$ and G(n, m) are independent of m. It will become evident that n = 111 is a critical direction, and we therefore rewrite E and ν in forms emphasizing this direction:

$$\frac{1}{E(\mathbf{n})} = \frac{1}{E_{111}} + \left[\frac{1}{3} - F(\mathbf{n}) \right] \chi, \quad \frac{\nu(\mathbf{n}, \mathbf{m})}{E(\mathbf{n})} = \frac{\nu_{111}}{E_{111}} + \left[\frac{1}{3} - D(\mathbf{n}, \mathbf{m}) \right] \frac{\chi}{2}, \quad (2.13)$$

where $E_{111} = E(111)$, $\nu_{111} = \nu(111, \cdot)$ and χ (Hayes & Shuvalov 1998) are

$$E_{111} = \left(\frac{1}{9\kappa} + \frac{1}{3\mu_1}\right)^{-1}, \quad \nu_{111} = \frac{3\kappa - 2\mu_1}{6\kappa + 2\mu_1}, \quad \chi = \frac{1}{\mu_2} - \frac{1}{\mu_1}. \tag{2.14}$$

Both E_{111} and ν_{111} are independent of μ_2 . The fact that $F \leq 1/3$ with equality for n = 111 implies that this is the only stretch direction for which E, and hence ν , are independent of μ_2 . Equations (2.13) indicate that E(n) and $\nu(n, m)$ depend on μ_2 at any point in the neighbourhood of 111, with particularly strong dependence if μ_2 is small. This singular behaviour is the reason for the extraordinary values of ν discovered by Ting & Chen (2005) and will be discussed at further length below after we have determined the global extrema for ν .

(c) Extreme values of G and ν for fixed n

For a given n, consider the defined vector

$$\boldsymbol{m}(\lambda) \equiv \rho\left(\frac{n_1}{n_1^2 - \lambda}, \frac{n_2}{n_2^2 - \lambda}, \frac{n_3}{n_3^2 - \lambda}\right),\tag{2.15}$$

with ρ chosen to make m a unit vector. Requiring $n \cdot m = 0$ implies that $m(\lambda)$ is orthogonal to n if

$$\frac{n_1^2}{n_1^2 - \lambda} + \frac{n_2^2}{n_2^2 - \lambda} + \frac{n_3^2}{n_3^2 - \lambda} = 0, \tag{2.16}$$

i.e. if λ is a root of the quadratic

$$\lambda^2 - 2\lambda(n_1^2 n_2^2 + n_2^2 n_3^2 + n_3^2 n_1^2) + 3n_1^2 n_2^2 n_3^2 = 0.$$
 (2.17)

It is shown in appendix A that the extreme values of D(n, m) for fixed n coincide with these roots, which are non-negative, and that the corresponding unit m vectors provide the extremal lateral directions. The basic result is described next.

(i) A fundamental result

Let $0 \le \lambda_{-} \le \lambda_{+} \le 1/2$ be the roots of (2.17) and m_{-} , m_{+} the associated vectors from (2.15), i.e.

$$\lambda_{\pm} = (n_1^2 n_2^2 + n_2^2 n_3^2 + n_3^2 n_1^2) \pm \sqrt{(n_1^2 n_2^2 + n_2^2 n_3^2 + n_3^2 n_1^2)^2 - 3n_1^2 n_2^2 n_3^2}, \quad (2.18a)$$

$$\mathbf{m}_{\pm} = \rho_{\pm} \left(\frac{n_1}{n_1^2 - \lambda_{\pm}}, \frac{n_2}{n_2^2 - \lambda_{\pm}}, \frac{n_3}{n_3^2 - \lambda_{\pm}} \right),$$
 (2.18b)

$$\rho_{\pm} = \left[\frac{n_1^2}{(n_1^2 - \lambda_{\pm})^2} + \frac{n_2^2}{(n_2^2 - \lambda_{\pm})^2} + \frac{n_3^2}{(n_3^2 - \lambda_{\pm})^2} \right]^{-1/2}.$$
 (2.18c)

The extreme values of D for a given \boldsymbol{n} are λ_{\pm} associated with the orthonormal triad $\{\boldsymbol{n}, \boldsymbol{m}_{-}, \boldsymbol{m}_{+}\}$, i.e.

$$D_{\min}(\mathbf{n}) = D(\mathbf{n}, \mathbf{m}_{-}) = \lambda_{-}, \quad D_{\max}(\mathbf{n}) = D(\mathbf{n}, \mathbf{m}_{+}) = \lambda_{+}.$$
 (2.19)

The extreme values of G and ν for fixed n follow from equations (2.5) and (2.6). The above result also implies that the extent of the variation of the shear modulus and the Poisson's ratio for a given stretch direction n are

$$1/G_{\min}(n) - 1/G_{\max}(n) = |\chi|4H(n), \qquad (2.20a)$$

$$\nu_{\text{max}}(\boldsymbol{n}) - \nu_{\text{min}}(\boldsymbol{n}) = |\chi|E(\boldsymbol{n})H(\boldsymbol{n}), \qquad (2.20b)$$

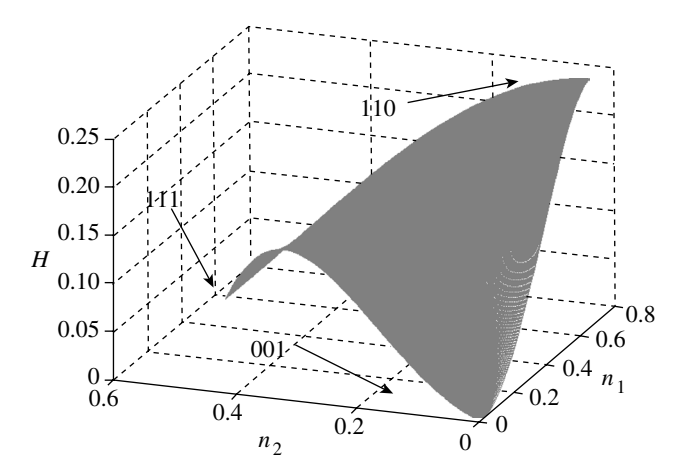


Figure 1. The function H of equation (2.21) plotted versus n_1 and n_2 for the region of solid angle depicted in figure 2. Vertices n = 111, 110 and 001 are indicated. H vanishes at 111 and 001 and is positive elsewhere, with maximum of 1/4 along n = 110 (face diagonals).

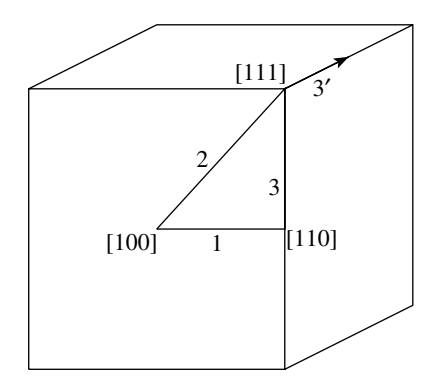


Figure 2. The irreducible 1/48th of the cube surface is defined by the isosceles triangle with edges 1, 2 and 3. The vertices opposite these edges correspond to, n = 111, 110 and 001, respectively. Note that the edge 3' is equivalent to 3 (which is used in appendix B).

where $H(\mathbf{n})$ is, see figure 1,

$$H(\mathbf{n}) = [(n_1^2 n_2^2 + n_2^2 n_3^2 + n_3^2 n_1^2)^2 - 3n_1^2 n_2^2 n_3^2]^{1/2}. \tag{2.21}$$

3. Poisson's ratio

We now consider the global extrema of $\nu(n, m)$ over all directions n and m. Two methods are used to derive the main results. The first uses general equations for a stationary value of ν in anisotropic media to obtain a single equation which must be satisfied if the stationary value lies in the interior of the triangle in figure 2. It is shown that this condition, which is independent of material parameters, is not satisfied, and hence all stationary values of ν in cubic materials lie on the edges of the triangle. This simplifies the problem considerably, and permits us to deduce

explicit relations for the stationary values. The second method, described in appendix B, confirms the first approach by a comprehensive numerical test of all possible material parameters.

(a) General conditions for stationary Poisson's ratio

General conditions can be derived which must be satisfied in order that Poisson's ratio is stationary in anisotropic elastic materials (Norris submitted). These are

$$s'_{14} = 0, \quad 2\nu s'_{15} + s'_{25} = 0, \quad (2\nu - 1)s'_{16} + s'_{26} = 0,$$
 (3.1)

where the stretch is in the 1' direction (n) and 2' is in the lateral direction (m). The conditions may be obtained by considering the derivative of ν with respect to rotation of the pair (n, m) about an arbitrary axis. Setting the derivatives to zero yields the stationary conditions (3.1).

The only non-zero contributions to s'_{14} , s'_{15} , s'_{25} , s'_{16} and s'_{26} in a material of cubic symmetry come from D. Thus, we may rewrite the conditions for stationary values of ν in terms of $D'_{14} = D'_{1123}$, etc. as

$$D'_{14} = 0$$
, $2\nu D'_{15} + D'_{25} = 0$, $(2\nu - 1)D'_{16} + D'_{26} = 0$. (3.2)

The first is automatically satisfied by virtue of the choice of the direction-m as either of m_+ . Regardless of which is chosen,

$$D_{14}' = D_{ijkl} n_i n_j m_{+k} m_{-l}$$

$$= \rho_{+}\rho_{-} \left[\frac{n_{1}^{4}}{(n_{1}^{2} - \lambda_{+})(n_{1}^{2} - \lambda_{-})} + \frac{n_{2}^{4}}{(n_{2}^{2} - \lambda_{+})(n_{2}^{2} - \lambda_{-})} + \frac{n_{3}^{4}}{(n_{3}^{2} - \lambda_{+})(n_{3}^{2} - \lambda_{-})} \right]$$
(3.3)
$$= 0.$$

The final identity may be derived by first splitting each term into partial fractions and using the following (cf. appendix A):

$$\frac{n_1^4}{n_1^2 - \lambda_{\pm}} + \frac{n_2^4}{n_2^2 - \lambda_{\pm}} + \frac{n_3^4}{n_3^2 - \lambda_{\pm}} = 1.$$
 (3.4)

With no loss in generality, consider the specific case of $\mathbf{m} = \mathbf{m}_a$, $\lambda = \lambda_a$, where $a = \pm$, and in either case, b = -a. It may be shown without much difficulty (appendix B) that $\rho_{\pm} > 0$ for \mathbf{n} in the interior of the triangle of figure 2. It then follows that inside the triangle,

$$\frac{D'_{15}}{\rho_b} = \frac{D'_{16}}{\rho_a} = 1, \quad \frac{D'_{25}}{\rho_b} = \frac{\lambda_a}{\lambda_a - \lambda_b}, \quad \frac{D'_{26}}{\rho_a} = \frac{\lambda_a}{\lambda_a - \lambda_b} - 2. \tag{3.5}$$

These identities may be obtained using partial fraction identities similar to those in equations (3.3) and (3.4). Equations $(3.2)_2$ and $(3.2)_3$ can be rewritten

$$\begin{bmatrix} D'_{15} & D'_{25} \\ D'_{16} & D'_{26} - D'_{16} \end{bmatrix} \begin{pmatrix} 2\nu \\ 1 \end{pmatrix} = \begin{pmatrix} 0 \\ 0 \end{pmatrix}. \tag{3.6}$$

However, using (3.5), the determinant of the matrix is

$$D'_{15}D'_{26} - (D'_{15} + D'_{25})D'_{16} = -3\rho_{+}\rho_{-}, \tag{3.7}$$

which is non-zero inside the triangle of figure 2. This gives us the important result: there are no stationary values of ν inside the triangle of figure 2. Hence, the only possible stationary values are on the edges.

(b) Stationary conditions on the triangle edges

The analysis above for the three conditions (3.2) is not valid on the triangle edges in figure 2, because the quantities ρ_{\pm} become zero and careful limits must be taken. We avoid this route by considering the conditions (3.2) afresh for n directed along the three edges. We find, as before, that $D'_{14} = 0$ on the three edges, so that (3.2)₁ always holds. Of the remaining two conditions, one is always satisfied, and imposing the other condition gives the answer sought.

The direction-n can be parametrized along each edge with a single variable. Thus, n = 1p0, $0 \le p \le 1$, on edge 1. Similarly, edges 2 and 3 are together covered by n = 11p, with $0 \le p < \infty$. In each case, we also need to consider the two possible values of m, which we proceed to do, focusing on the conditions $(3.2)_2$ and $(3.2)_3$.

(i) Edge 1: n = 1p0, $0 \le p \le 1$ and $m = p\bar{1}0$ or 001

For $m = p\bar{1}0$, we find that $D'_{15} = D'_{25} = 0$ and $D'_{16} = -D'_{26} = p - p^3$. Hence, equation $(3.2)_2$ is automatically satisfied, while equation $(3.2)_3$ becomes

$$(\nu - 1)(p - p^3) = 0. (3.8)$$

Conversely, for m = 001 it turns out that $D'_{16} = D'_{26} = 0$ and $D'_{15} = -D'_{25} = p - p^3$. In this case, the only non-trivial equation from equations (3.2) is the second one,

$$\nu(p - p^3) = 0. (3.9)$$

Apart from the specific cases $\nu=0$ or 1, equations (3.8) and (3.9) imply that stationary values of ν occur only at the end points p=0 and 1. Thus, $\nu(001)$, $\nu(110,1\bar{1}0)$ and $\nu(110,001)$ are potential candidates for global extrema of ν .

(ii) Edges 2 and 3: n = 11p, $0 \le p < \infty$ and $m = 1\overline{1}0$

Proceeding as before, we find that $D'_{16}=D'_{26}=0$, $D'_{15}=\sqrt{2}p(1-p^2)/(2+p^2)^2$ and $D'_{25}=p/[\sqrt{2}(2+p^2)]$. Hence, equation (3.2)₃ is automatically satisfied, while equation (3.2)₂ becomes

$$p[(1-4\nu)p^2 + 2 + 4\nu] = 0. (3.10)$$

The zero p=0 corresponds to n=110 which was considered above. Thus, all three conditions (3.2) are met if p is such that

$$p^{2} = (\nu + 1/2)/(\nu - 1/4). \tag{3.11}$$

Further progress is made using the representation of equation (2.13) combined with the limiting values of D which can be easily evaluated. We find

$$\frac{E_{111}}{E_{11p}} = 1 + \frac{1}{3} \left(\frac{1 - p^2}{2 + p^2} \right)^2 E_{111} \chi, \tag{3.12a}$$

$$\nu(11p, 1\bar{1}0) \frac{E_{111}}{E_{11p}} = \nu_{111} - \frac{1}{6} \left(\frac{1 - p^2}{2 + p^2} \right) E_{111} \chi. \tag{3.12b}$$

Substituting for p^2 from equation (3.11) into (3.12) gives two coupled equations for E_{11p} and $\nu(11p, 1\bar{1}0)$:

$$\frac{1}{E_{11p}} = \frac{1}{E_{111}} + \frac{\chi}{48\nu^2}, \quad \frac{\nu}{E_{11p}} = \frac{\nu_{111}}{E_{111}} + \frac{\chi}{24\nu}.$$
 (3.13)

Eliminating E_{11p} yields a single equation for possible stationary values of $\nu(11p, 1\bar{1}0)$,

$$\nu^2 - \nu \nu_{111} - \frac{1}{48} E_{111} \chi = 0. \tag{3.14}$$

We will return to this after considering the other possible m vector.

(iii) Edges 2 and 3: $\mathbf{m} = pp\bar{2}$

In this case $D'_{15} = D'_{25} = 0$, $D'_{16} = \sqrt{2}p(1-p^2)/(2+p^2)^2$ and $D'_{26} = p(p^2-4)/(\sqrt{2}(2+p^2)^2)$. Equation (3.2)₂ holds, while equation (3.2)₃ is zero if p=0, which is disregarded, or if p is such that

$$p^{2} = (\nu - 3/2)/(\nu - 3/4). \tag{3.15}$$

The Young modulus is independent of m and given by (3.12a), while ν satisfies

$$\nu(11p, pp\bar{2})\frac{E_{111}}{E_{11p}} = \nu_{111} + \frac{(1-p^2)(4-p^2)}{6(2+p^2)^2}E_{111}\chi.$$
 (3.16)

Using the value of p^2 from (3.15) in equations (3.12a) and (3.16) yields another pair of coupled equations, for E_{11p} and $\nu(11p,001)$,

$$\frac{1}{E_{11p}} = \frac{1}{E_{111}} + \frac{\chi}{48(\nu - 1)^2}, \quad \frac{\nu}{E_{11p}} = \frac{\nu_{111}}{E_{111}} + \frac{\chi(\nu - \frac{1}{2})}{24(\nu - 1)^2}.$$
 (3.17)

These imply a single equation for possible stationary values of $\nu(11p,001)$,

$$(\nu - 1)^2 - (\nu - 1)(\nu_{111} - 1) - \frac{1}{48}E_{111}\chi = 0.$$
(3.18)

(c) Definition of v_1 and v_2

The analysis for the three edges gives a total of seven candidates for global extrema: $\nu(001)$, $\nu(110,1\bar{1}0)$ and $\nu(110,001)$ from the endpoints of edge 1, and the four roots of equations (3.14) and (3.18) along edges 2 and 3. The latter are very interesting because they are the only instances of possible extreme values

associated with directions other than the principal directions of the cube (axes, face diagonals). Results below will show that five of the seven candidates are global extrema, depending on the material properties. These are $\nu(001)$, $\nu(110,1\bar{1}0)$, $\nu(110,001)$ and the following two distinct roots of equations (3.14) and (3.18), respectively,

$$\nu_1 \equiv \frac{1}{2}\nu_{111} - \frac{1}{2}\sqrt{\nu_{111}^2 + \frac{1}{6}(\nu_{111} + 1)\left(\frac{\mu_1}{\mu_2} - 1\right)},\tag{3.19a}$$

$$\nu_2 \equiv \frac{1}{2}(\nu_{111} + 1) + \frac{1}{2}\sqrt{(\nu_{111} - 1)^2 + \frac{1}{6}(\nu_{111} + 1)\left(\frac{\mu_1}{\mu_2} - 1\right)}.$$
 (3.19b)

The quantity $E_{111}\chi$ has been replaced to emphasize the dependence upon the two parameters ν_{111} and the anisotropy ratio μ_1/μ_2 . The associated directions follow from equations (3.11) and (3.15),

$$\nu_1 = \nu(11p_1, 1\bar{1}0), \quad p_1 = \left(\frac{\nu_1 + 1/2}{\nu_1 - 1/4}\right)^{1/2},$$
 (3.20a)

$$\nu_2 = \nu(11p_2, p_2p_2\bar{2}), \quad p_2 = \left(\frac{\nu_2 - 3/2}{\nu_2 - 3/4}\right)^{1/2}.$$
 (3.20b)

A complete analysis is provided in appendix B. At this stage, we note that ν_1 is identical to the minimum value of ν deduced by Ting & Chen (2005), i.e. eqns (4.13) and (4.15) of their paper, with the minus sign taken in eqn (4.13).

4. Material properties in terms of Poisson's ratios

Results for the global extrema are presented after we introduce several quantities.

(a) Non-dimensional parameters

It helps to characterize the Poisson's ratio in terms of two non-dimensional material parameters which we select as ν_0 and χ_0 , where

$$\nu_0 = \frac{3\kappa - 2\mu_2}{6\kappa + 2\mu_2}, \quad \chi_0 = \frac{\mu_2^{-1} - \mu_1^{-1}}{(9\kappa)^{-1} + (3\mu_2)^{-1}}.$$
 (4.1)

That is, $\nu_0 = -s_{12}/s_{11}$ is the axial Poisson's ratio $\nu(001, \cdot)$, independent of the orthogonal direction, and $\chi_0 = \chi/s_{11}$ is the non-dimensional analogue of χ . Thus,

$$\nu(\boldsymbol{n}, \boldsymbol{m}) = \frac{\nu_0 - \frac{1}{2} \chi_0 D(\boldsymbol{n}, \boldsymbol{m})}{1 - \chi_0 F(\boldsymbol{n})}, \tag{4.2}$$

a form which shows clearly that ν is negative (positive) for all directions if $\nu_0 < 0$ and $\chi_0 > 0$ ($\nu_0 > 0$ and $\chi_0 < 0$). These conditions for cubic materials to be completely auxetic (non-auxetic) were previously derived by Ting & Barnett (2005).

The extreme values of the Poisson's ratio for a given n are

$$\nu_{\pm}(\mathbf{n}) = \frac{\nu_0 - \frac{1}{2}\chi_0(F \pm H)}{1 - \chi_0 F},\tag{4.3}$$

where F is defined in (2.7) and H in (2.21). Thus, ν_+ is the minimum (maximum) and ν_- the maximum (minimum) if $\chi_0 > 0$ ($\chi_0 < 0$), respectively.

The Poisson's ratio is a function of the direction pair (n, m) and the material parameter pair (ν_0, χ_0) , i.e. $\nu = \nu(n, m, \nu_0, \chi_0)$. The dependence upon ν_0 has an interesting property: for any orthonormal triad,

$$\nu(n, m, \nu_0, \chi_0) + \nu(n, t, 1 - \nu_0, \chi_0) = 1. \tag{4.4}$$

This follows from (4.2) and the identities (2.8). Result (4.4) will prove useful later.

Several particular values of Poisson's ratio have been introduced: $\nu_0 = \nu(001, \boldsymbol{m}), \ \nu_{111} = \nu(111, \boldsymbol{m})$ associated with the two directions 001 and 111 for which ν is independent of \boldsymbol{m} . These are two vertices of the triangle in figure 2. At the third vertex $(\boldsymbol{n} = 110 \text{ along the face diagonals})$, we have $\nu(110, \boldsymbol{m}) = m_3^2 \nu_{001} + (1 - m_3^2) \nu_{1\bar{1}0}$ where, in the notation of (Milstein & Huang 1979) $\nu_{001} \equiv \nu(110,001)$ and $\nu_{1\bar{1}0} \equiv \nu(110,1\bar{1}0)$. Three of these four values of Poisson's ratio associated with principal directions can be global extrema, and the fourth, ν_{111} plays a central role in the definition of ν_1 and ν_2 of (3.19). We therefore consider them in terms of the non-dimensional parameters ν_0 and χ_0 ,

$$\nu_{111} = \frac{\nu_0 - \frac{1}{6}\chi_0}{1 - \frac{1}{3}\chi_0}, \quad \nu_{001} = \frac{\nu_0}{1 - \frac{1}{4}\chi_0}, \quad \nu_{1\bar{1}0} = \frac{\nu_0 - \frac{1}{4}\chi_0}{1 - \frac{1}{4}\chi_0}. \tag{4.5}$$

We return to ν_1 and ν_2 later.

(b) Positive definiteness and Poisson's ratios

In order to summarize the global extrema of ν , we first need to consider the range of possible material parameters. It may be shown that the requirements for the strain energy to be positive definite: $\kappa > 0$, $\mu_2 > 0$ and $\mu_1 > 0$, can be expressed in terms of ν_0 and χ_0 as

$$-1 < \nu_0 < 1/2, \quad \chi_0 < 2(1 + \nu_0).$$
 (4.6)

It will become evident that the global extrema for ν depend most simply on the two values for \boldsymbol{n} along a face diagonal: ν_{001} and $\nu_{1\bar{1}0}$. The constraints (4.6) become

$$-1 < \nu_{1\bar{1}0} < 1, \quad -\frac{1}{2} (1 - \nu_{1\bar{1}0}) < \nu_{001} < 1 - \nu_{1\bar{1}0}, \tag{4.7}$$

which define the interior of a triangle in the $\nu_{001}, \nu_{1\bar{1}0}$ plane, see figure 3. This figure also indicates the lines $\nu_0=0$ and $\chi_0=0$ (isotropy). It may be checked that the four quantities $\{\nu_0,\nu_{111},\nu_{001},\nu_{1\bar{1}0}\}$ are different as long $\chi_0\neq 0$, with the exception of ν_{001} and ν_0 which are distinct if $\nu_0\chi_0\neq 0$. Consideration of the four possibilities yields the ordering

$$0 < \nu_{001} < \nu_0 < \nu_{111} < \nu_{1\bar{1}0} < 1 \quad \text{for } \nu_0 > 0, \ \chi_0 < 0, \tag{4.8a}$$

$$-1 < \nu_0 < \nu_{001} < \nu_{111} < \nu_{1\bar{1}0} < 0 \quad \text{for } \nu_0 < 0, \ \chi_0 < 0, \tag{4.8b}$$

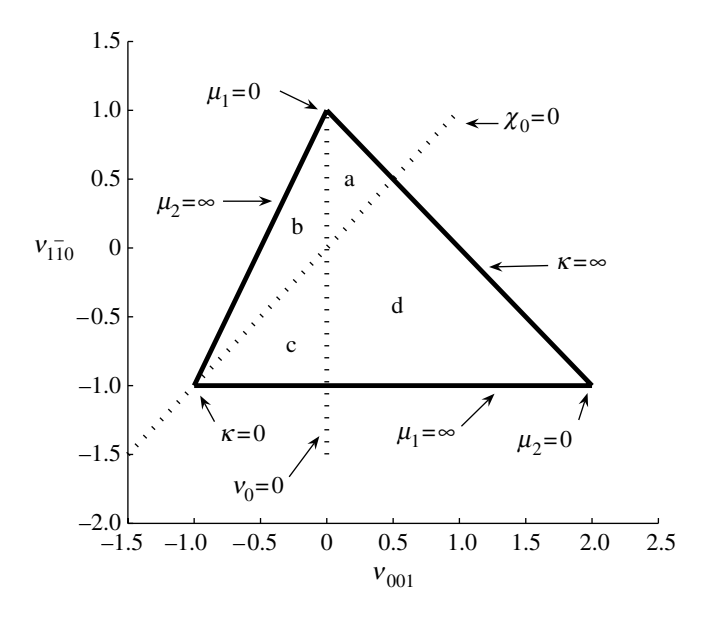


Figure 3. The interior of the triangle in the ν_{001} , $\nu_{1\bar{1}0}$ plane represents the entirety of possible cubic materials with positive definite strain energy. The vertices correspond to $\kappa=0$, $\mu_1=0$ and $\mu_2=0$, as indicated. The edges of the triangle opposite the vertices are the limiting cases in which κ^{-1} , μ_1^{-1} and μ_2^{-1} vanish, respectively. The dashed curves correspond to $\nu_0=0$ (vertical) and $\chi_0=0$ (diagonal) and the regions a, b, c and d defined by these lines coincide with the four cases in equation (4.8), respectively.

$$-1 < \nu_{1\bar{1}0} < \nu_{111} < \nu_{001} < \nu_0 < 0 \quad \text{for } \nu_0 < 0, \ \chi_0 > 0, \tag{4.8c}$$

$$0 < \nu_{1\bar{1}0} < \nu_{111} < \nu_0 < \nu_{001} < 2 \quad \text{for } \nu_0 > 0, \ \chi_0 > 0.$$
 (4.8*d*)

Note that ν_{111} is never a maximum or minimum. We will see below that (4.8a) is the only case for which the extreme values coincide with the global extrema for ν . This is one of the reasons the classification of the extrema for ν is relatively complicated, requiring that we identify several distinct values. In particular, the global extrema depend upon more than $\operatorname{sgn} \nu_0$ and $\operatorname{sgn} \chi_0$, but are best characterized by the two independent non-dimensional parameters ν_{001} and $\nu_{1\bar{1}0}$. We are now ready to define the global extrema.

5. Minimum and maximum Poisson's ratio

Tables 1 and 2 list the values of the global minimum ν_{\min} and the global maximum ν_{\max} , respectively, for all possible combinations of elastic parameters. For table 1, $\nu(001)$, ν_{001} and $\nu_{1\bar{1}0}$ are defined in (4.5), and ν_1 and p_1 are defined in (3.19a) and (3.20a). For table 2, ν_2 and p_2 are defined in (3.19b) and (3.20b). No second condition is necessary to define the region for case e, which is clear from figure 5. The data in tables 1 and 2 are illustrated in figures 4 and 5, respectively, which define the global extrema for every point in the interior of the triangle

$ u_{ m min}$	n	m	condition 1	condition 2	figure 4
$\begin{array}{l} 0 < \nu_{001} \\ -1/2 < \nu_{1\bar{1}0} \\ -1 < \nu_{0} \\ -\infty < \nu_{1} \end{array}$	110 110 001 $11p_1$	001 $1\overline{10}$ arbitrary $1\overline{10}$	$\begin{array}{l} \nu_{001} > 0 \\ \nu_{1\bar{1}0} > -1/2 \\ \nu_{001} < 0 \\ \nu_{1\bar{1}0} < -1/2 \end{array}$	$egin{array}{l} u_{1ar{1}0} > u_{001} \\ u_{1ar{1}0} < u_{001} \\ u_{1ar{1}0} > u_{001} \\ u_{1ar{1}0} < u_{001} \end{array}$	a b c d

Table 1. The global minimum of Poisson's ratio for cubic materials.

Table 2. The global maximum of Poisson's ratio.

$ u_{ m max}$	n	m	condition 1	condition 2	figure 5
$v_1 < -1/2$	$11p_{1}$	$1\bar{1}0$	$\nu_{1\bar{1}0} < -1/2$	$\nu_{1\bar{1}0} > \nu_{001}$	a
$\nu_0 < 0$	001	arbitrary	$v_{001} < 0$	$v_{1\bar{1}0} < v_{001}$	b
$\nu_{1\bar{1}0} < 1$	110	$1\bar{1}0$	$\nu_{1\bar{1}0} > -1/2$	$\nu_{1\bar{1}0} > \nu_{001}$	\mathbf{c}
$\nu_{001} < 3/2$	110	001	$0 < \nu_{001} < 3/2$	$\nu_{1\bar{1}0} < \nu_{001}$	d
$\nu_2 < \infty$	$11p_2$	$p_2p_2\bar{2}$	$\nu_{001} > 3/2$		e

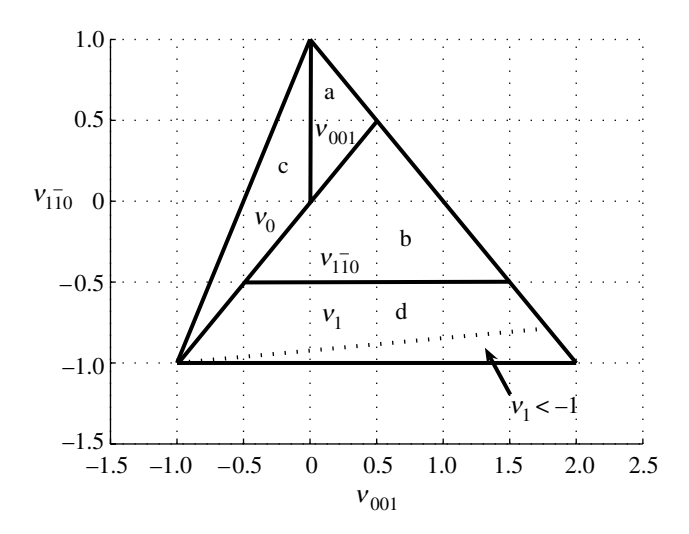


Figure 4. The global minimum of Poisson's ratio based on table 1. The value of $\nu_{\rm min}$ depends upon the location of the cubic material parameters in the four distinct regions a, b, c and d, defined by the heavy lines inside the triangle of possible materials. The diagonal dashed line delineates the region in which $\nu_{\rm min} < -1$, from equation (5.1).

defined by (4.7). The details of the analysis and related numerical tests leading to these results are presented in appendix B.

(a) Discussion

Conventional wisdom prior to Ting & Chen (2005) was that the extreme values were characterized by the face diagonal values ν_{001} and $\nu_{1\bar{1}0}$. But as equation (4.8) indicates, even these are not always extrema, since $\nu_0 = \nu(001, m)$

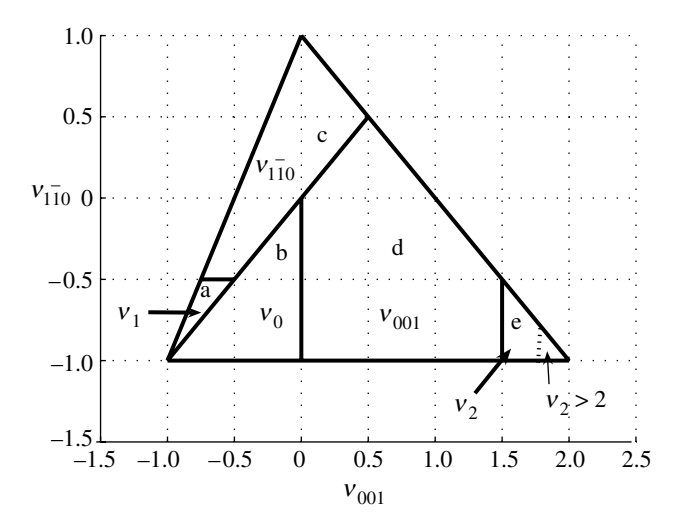


Figure 5. The global maximum of Poisson's ratio based on table 2. The value of ν_{max} depends upon the location of $(\nu_{001}, \nu_{1\bar{1}0})$ in five distinct regions defined by the heavy lines. The dashed line delineates the (small) region in which $\nu_{\text{max}} > 2$, from equation (5.1).

can be maximum or minimum under appropriate circumstances (equations (4.8c) and (4.8d), respectively). The extreme values in equation (4.8) are all bounded by the limits of the triangle in figure 3. Specifically, they limit the Poisson's ratio to lie between -1 and 2. Ting & Chen (2005) showed by explicit demonstration that this is not the case, and that values less than -1 and larger than 2 are feasible, and remarkably, no lower or upper limits exist for ν .

The Ting & Chen 'effect' occurs in figure 4 in the region, where $\nu_{\min} = \nu_1$ and in figure 5 in the region $\nu_{\max} = \nu_2$. Using equation (3.19a), we can determine that ν_{\min} is strictly less than -1 if $(\mu_1/\mu_2-1)>24$. Similarly, equation (3.19b) implies that ν_{\max} is strictly greater than 2 if $(\mu_1/\mu_2-1)(\nu_{111}+1)>24(2-\nu_{111})$. By converting these inequalities, we deduce

$$\nu_{\min} < -1 \quad \Leftrightarrow \quad \mu_2 < \frac{\mu_1}{25} \quad \Leftrightarrow \quad \nu_{001} - 13 \\ \nu_{1\bar{1}0} > 12, \qquad (5.1a)$$

$$\nu_{\text{max}} > 2 \iff \mu_2 < \left(\frac{25}{\mu_1} + \frac{16}{\kappa}\right)^{-1} \iff 13\nu_{001} - \nu_{1\bar{1}0} > 24.$$
 (5.1b)

The two sub-regions defined by the ν_{001} , $\nu_{1\bar{1}0}$ inequalities are depicted in figures 4 and 5. They define neighbourhoods of the $\mu_2 = 0$ vertex, i.e. $(\nu_{001}, \nu_{1\bar{1}0}) = (2, -1)$, where the extreme values of ν can achieve arbitrarily large positive and negative values. The condition for $\nu_{\min} < -1$ is independent of the bulk modulus κ . Thus, the occurrence of negative values of ν less than -1 does not necessarily imply that relatively large positive values (greater than 2) also occur, but the converse is true. This is simply a consequence of the fact that the dashed region near the tip $\mu_2 = 0$ in figure 5 is contained entirely within the dashed region of figure 4.

These results indicate that the necessary and sufficient condition for the occurrence of large extrema for ν is that μ_2 is much less than either μ_1 or κ . μ_2 is either the maximum or minimum of G, and it is associated with directions pairs

Table 3. Properties of the 11 materials of cubic symmetry in figure 6 with $\nu_{1\bar{1}0} < -1/2$. (The
boldfaced numbers indicate $\nu_{\rm min}$ and $\nu_{\rm max}.$ Unless otherwise noted the data are from Landolt &
Bornstein (1992). G&S indicates Gunton & Saunders (1975).)

material	v_{001}	$v_{1\bar{1}0}$	ν_1	p_1	ν_2	p_2	μ_1/μ_2
β-brass (Musgrave 2003)	1.29	-0.52	-0.52	0.15			8.5
Li	1.29	-0.53	-0.54	0.21			8.8
AlNi (at 63.2% Ni and at 273 K)	1.28	-0.55	-0.55	0.25			9.1
CuAlNi (Cu14% Al4.1% Ni)	1.37	-0.58	-0.59	0.32			10.2
CuAlNi (Cu14.5% Al3.15% Ni)	1.41	-0.63	-0.66	0.42			12.1
CuAlNi	1.47	-0.65	-0.69	0.45			13.1
AlNi (at 60% Ni and at 273 K)	1.53	-0.68	-0.74	0.50	1.53	0.18	15.0
InTl (at 27% Tl, 290 K) (G&S)	1.75	-0.78	-0.98	0.62	1.89	0.59	24.0
InTl (at 28.13% Tl)	1.78	-0.81	-1.08	0.66	2.00	0.63	28.6
InTl (at 25% Tl)	1.82	-0.84	-1.21	0.70	2.14	0.68	34.5
InTl (at 27% Tl, 200 K) (G&S)	1.93	-0.94	-2.10	0.83	3.01	0.82	90.9

requires that this shear modulus is much less than $\mu_1 = G(001, \mathbf{m})$, and much less than the bulk modulus κ . In the limit of very small μ_2 , equations (3.19) give $\nu_{1,2} \approx \mp \sqrt{(\nu_{111}+1)\mu_1/(24\mu_2)}$. Ting (2004) found that the extreme values are $\nu \approx \pm \sqrt{3/(16\delta)} + \mathrm{O}(1)$ for small values of their parameter δ . In current notation, this is $\delta = 9/[1+E_{111}\chi]$, and replacing $E_{111}\chi$ the two theories are seen to agree. The implications of small μ_2 for Young's modulus are apparent. Thus, $E_{\min}/E_{\max} = O(\mu_2/\mu_1)$, and equation (2.13)₁ indicates that $E(\mathbf{n})$ is small everywhere except near the 111-direction, at which it reaches a sharply peaked maximum. Cazzani & Rovati (2003) provide numerical examples illustrating the directional variation of E for a range of cubic materials, some of which are considered below. Their three-dimensional plots of $E(\mathbf{n})$ for materials with very large values of μ_1/μ_2 (see table 3 below) look like very sharp starfish. Although, the directions at which ν_1 and ν_2 are large in magnitude are close to the 111-direction, the value of E in the stationary directions can be quite different from

 E_{111} . The precise values of the Young modulus, E_{11p_1} and E_{11p} at the associated

along orthogonal face diagonals, $\mu_2 = G(110, 1\bar{1}0)$. Hence, the Ting & Chen effect

$$\frac{E_{111}}{E_{11p_1}} + \frac{\nu_{111}}{\nu_1} = 2, \quad \frac{E_{111}}{E_{11p_2}} + \frac{\nu_{111} - 1}{\nu_2 - 1} = 2. \tag{5.2}$$

These identities, which follow from equations (3.13) and (3.17), respectively, indicate that if ν_1 or ν_2 become large in magnitude then the second term in the left member is negligible. The associated value of the Young modulus is approximately one half of the value in the 111-direction and consequently large values of $|\nu|$ occur in directions at which $E \approx (1/2)E_{111}$. Such directions, by their nature, are close to 111.

The appearance of ν_1 in both figures 4 and 5 is not surprising if one considers that ν_{001} , $\nu_{1\bar{1}0}$ and ν_0 also occur in both the minimum and maximum. It can be checked that in the region where ν_1 is the maximum value in figure 5, it satisfies $-1 < \nu_1 < -1/2$. In fact, it is very close to but not equal to

stretch directions are given by

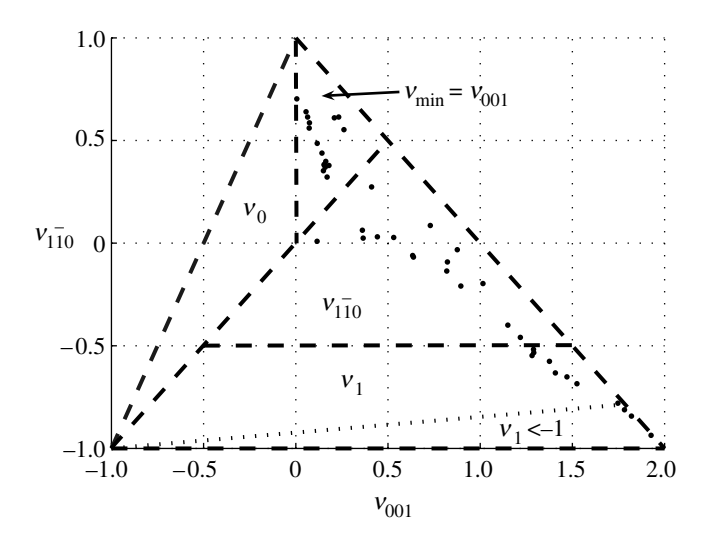


Figure 6. The 44 materials considered are indicated by dots on the chart showing the ν_{\min} regions, cf. figure 4.

 $\nu_{1\bar{1}0}$ in this region, and numerical results indicate that $|\nu_1 - \nu_{1\bar{1}0}| < 4 \times 10^{-4}$ in this small sector.

What is special about the transition values in figures 4 and 5: $\nu_{001} = 3/2$ and $\nu_{1\bar{1}0} = -1/2$? Quite simply, they are the values of ν_1 and ν_2 as the stationary directions \boldsymbol{n} approach the face diagonal direction-110. Thus, ν_1 and ν_2 are both the continuation of the face diagonal value $\nu_{1\bar{1}0}$, but on two different branches. See appendix B for further discussion.

(b) Application to cubic materials

We conclude by considering elasticity data for 44 materials with cubic symmetry, figure 6. The data are from Musgrave (2003) unless otherwise noted. The 17 cubic materials in the region, where $\nu_{\min} = \nu_{001}$ are as follows, with the coordinates $(\nu_{001}, \nu_{1\bar{1}0})$ for each: GeTeSnTe¹ (mol% GeTe=0) (0.01, 0.70), RbBr¹ (0.06, 0.64), KI (0.06, 0.61), KBr (0.07, 0.59), KCl $(0.07, 0.56), \text{ Nb}^1 (0.21, 0.61), \text{ AgCl } (0.23, 0.61), \text{ KFl } (0.12, 0.49), \text{ CsCl}$ (0.18, 0.38), NaFl (0.17, 0.32). This lists them roughly in the order from top left to lower right. Note that all the materials considered have positive ν_{001} . The 16 materials with $\nu_{\rm min} = \nu_{001}$ also have $\nu_{\rm max} = \nu_{1\bar{1}0}$, so the coordinates of the above materials correspond to their extreme values of ν . The extreme values are also given by the coordinates in the region with $\nu_{\min} = \nu_{1\bar{1}0}$, $\nu_{\text{max}} = \nu_{001}$. The materials there are: Al (0.41, 0.27), diamond (0.12, 0.01), Si (0.36, 0.06), Ge (0.37, 0.02), GaSb (0.44, 0.03), InSb (0.53, 0.03), CuAu¹ (0.73, 0.09), Fe (0.63, -0.06), Ni (0.64, -0.07), Au (0.88, -0.03), Ag (0.82, -0.09), Cu (0.82, -0.14), α -brass (0.90, -0.21), Pb¹ (1.02, -0.20), Rb^1 (1.15, -0.40), Cs^1 (1.22, -0.46).

¹Data from Landolt & Bornstein (1992), see also Cazzani & Rovati (2003).

Materials with $\nu_{1\bar{1}0} < -1/2$ are listed in table 3. These all lie within the region where the minimum is ν_1 , and of these, five materials are in the sub-region where the maximum is ν_2 . Three materials are in the sub-regions with $\nu_1 < -1$ and $\nu_2 > 2$. These indium thallium alloys of different composition and at different temperatures are close to the stability limit where they undergo a martensitic phase transition from face-centred cubic form to face-centred tetragonal. The transition is discussed by, for instance, Gunton & Saunders (1975), who also provide data on another even more auxetic sample: InTl (at 27% Tl, 125 K). This material is so close to the $\mu_2 = 0$ vertex, with $\nu_{001} = 1.991$, $\nu_{1\bar{1}0} = -0.997$ and $\mu_1/\mu_2 = 1905$ (!) that we do not include it in the table or the figure for being too close to the phase transition, or equivalently, too unstable (it has $\nu_1 = -7.92$ and $\nu_2 = 8.21$).

We note that the stretch directions for the extremal values of ν , defined by $n=11p_1$ and $11p_2$, are distinct. As the materials approach the $\mu_2=0$ vertex, the directions coalesce as they tend towards the cube diagonal 111. The three materials in table 3 with $\nu_{\min} < -1$ and $\nu_{\max} > 2$ are close to the incompressibility limit, the line $\kappa = \infty$ in figure 3. In this limit, the averaged Poisson's ratio is $\bar{\nu}(n) = 1/2$, and therefore those Poisson's ratios which are independent of m tend to 1/2, i.e. $\nu_{111} = \nu_0 = 1/2$. Also, $\nu_{001} + \nu_{1\bar{1}0} = 1$ and $\nu_1 + \nu_2 = 1$, with

$$\nu_1 = \frac{1}{4} - \frac{1}{4} \sqrt{\frac{\mu_1}{\mu_2}}, \quad \nu_2 = \frac{3}{4} + \frac{1}{4} \sqrt{\frac{\mu_1}{\mu_2}}, \quad p_1 = p_2 = \sqrt{1 - 3\sqrt{\frac{\mu_2}{\mu_1}}}, \quad \kappa \to \infty. \quad (5.3)$$

These are reasonable approximations for the last three materials in table 3, which clearly satisfy $\nu_1 + \nu_2 \approx 1$ and $p_1 \approx p_2$.

6. Summary

Figures 4 and 5 along with tables 1 and 2 are the central results which summarize the extreme values of Poisson's ratio for all possible values of the elastic parameters for solids with positive strain energy and cubic material symmetry. The application of the related formulae to the materials in figure 6 shows that values less than -1 and greater than +2 are associated with certain stretch directions in some indium thallium alloys.

Discussions with Prof. T.C.T. Ting are appreciated.

Appendix A. Extreme values of D(n, m) for a given n

The extreme values of D(n, m) as a function of m for a given direction-n can be determined using Lagrange multipliers λ, ρ , and the generalized function

$$f(\mathbf{m}) = D(\mathbf{n}, \mathbf{m}) - \lambda |\mathbf{m}|^2 - 2\rho \mathbf{n} \cdot \mathbf{m}. \tag{A 1}$$

Setting to zero, the partial derivatives of f with respect to m_1 , m_2 , m_3 , implies three equations, which may be solved to give

$$\boldsymbol{m} = \left(\frac{\rho n_1}{n_1^2 - \lambda}, \frac{\rho n_2}{n_2^2 - \lambda}, \frac{\rho n_3}{n_3^2 - \lambda}\right),\tag{A 2}$$

where λ, ρ follow from the constraints $\boldsymbol{n} \cdot \boldsymbol{m} = 0$ and $|\boldsymbol{m}|^2 = 1$. These are, respectively, (2.16) and

$$\left[\frac{n_1^2}{(n_1^2 - \lambda)^2} + \frac{n_2^2}{(n_2^2 - \lambda)^2} + \frac{n_3^2}{(n_3^2 - \lambda)^2} \right] \rho^2 = 1.$$
 (A 3)

Equation (2.16) implies that λ is a root of the quadratic (2.17) and (A 3) yields the normalization factor ρ . These results are summarized in (2.18) and (2.19).

It may be easily checked that the function f is zero at the extremal values of D. But $f = D - \lambda$, and hence the extreme values of D(n, m) are simply the two roots of the quadratic (2.17), $0 \le \lambda_{-} \le \lambda_{+} \le 1/2$. Note that the extreme values depend only upon the invariants of the tensor **M** with components $M_{ii} = D_{iikl}n_kn_l$. Although this is a second-order tensor and normally possesses three independent invariants, one is trivially a constant: tr M = 1. The others are, e.g. tr $M^2 = n_1^4 +$ $n_2^4 + n_3^4 = 1 - 2F(\boldsymbol{n})$ (see equation (2.8)) and det $\mathbf{M} = n_1^2 n_2^2 n_3^2$. The above formulation is valid as long as $(n_1^2 - n_2^2)(n_2^2 - n_3^2)(n_3^2 - n_1^2) \neq 0$. For

instance, if $n_2^2 = n_1^2$, then $\lambda_-, \lambda_+ = \min, \max(n_1^2, 3n_1^2n_3^2)$. The \boldsymbol{m} vector associated with $\lambda = n_1^2$ is undefined, according to (A 2). However, by taking the limit $n_2^2 \to n_1^2$ it can be shown that $m \to \pm (1, -1, 0)/\sqrt{2}$. The other vector corresponding to $\lambda = 3n_1^2n_3^2$ has no such singularity, and is $m = \pm (n_3, n_3, -2n_1)/\sqrt{2}$. The identity (3.4) may be obtained by noting that each term can be split, e.g. $n_1^4/(n_1^2-\lambda) = n_1^2 + \lambda/(n_1^2-\lambda)$, then using the fundamental relation (2.16) with

 $n_1^2 + n_2^2 + n_3^2 = 1$. Various other identities can be found, e.g.

$$\frac{n_1^6}{(n_1^2 - \lambda_+)(n_1^2 - \lambda_-)} + \frac{n_2^6}{(n_2^2 - \lambda_+)(n_1^2 - \lambda_-)} + \frac{n_3^6}{(n_3^2 - \lambda_+)(n_1^2 - \lambda_-)} = 1.$$
 (A 4)

Appendix B. Analysis

Here, we derive stationary conditions for directions n along the edges of the triangle in figure 2 by direct analysis. Numerical tests are performed for the entire range of material parameters. The results are consistent with and reinforce those of §3.

The limiting Poisson's ratios of (4.3) are expressed $\nu_{+}(n) \equiv \nu_{+}(\alpha, \beta)$ in terms of two numbers, where

$$n_1^2 = (1+\alpha)\left(\frac{1}{3}-\beta\right), \quad n_2^2 = (1-\alpha)\left(\frac{1}{3}-\beta\right), \quad n_3^2 = \frac{1}{3}+2\beta.$$
 (B 1)

The range of (α, β) which needs to be considered is $0 \le \alpha \le 1$, $(\alpha/3(3+\alpha)) \le$ $\beta \leq 1/3$, corresponding to the triangle in figure 2. This parametrization allows quick numerical searching for global extreme values of ν for a given cubic material.

We first consider the three edges as shown in figure 2 in turn. Edge 1 is defined by $\alpha=1, 1/12 \le \beta \le 1/3$. The limiting values are $\nu_{-}(1,\beta)=\nu_{0}/[1-((1/3)-\beta)\times$ $((1/3) + 2\beta)2\chi_0$ and $\nu_+(1,\beta) = 1 - \nu_-(1,\beta)(1-\nu_0)/\nu_0$. The extreme values are obtained at the ends: $\nu_{-}(1,1/12) = \nu_{001}, \ \nu_{+}(1,1/12) = \nu_{1\bar{1}0}, \ \nu_{-}(1,1/3) =$ $\nu_{+}(1,1/3) = \nu_{0}$. These possible global extreme values agree with those of §3.

Inspection of figure 2 shows that edges 2 and 3 can be considered by looking at $\nu_{\pm}(0,\beta)$ for $-1/6 \le \beta \le 1/3$. Straightforward calculation gives

$$\nu_{-}(0,\beta) = \frac{\nu_{0} - \frac{1}{2} \left(\frac{1}{3} - \beta\right) \chi_{0}}{1 - \left(\frac{1}{3} - 3\beta^{2}\right) \chi_{0}}, \quad \nu_{+}(0,\beta) = \frac{\nu_{0} - \frac{1}{2} \left(\frac{1}{3} - \beta\right) (1 + 6\beta) \chi_{0}}{1 - \left(\frac{1}{3} - 3\beta^{2}\right) \chi_{0}}.$$
 (B 2)

A function of the form f/g is stationary at f/g = f'/g'. Applying this to the expressions in (B 2) implies that the extreme values of ν_- and ν_+ satisfy, respectively,

$$\nu_{-}(0,\beta) = \frac{1}{12\beta}, \quad \nu_{+}(0,\beta) = 1 - \frac{1}{12\beta}.$$
 (B 3)

Combining equations (B 2) and (B 3) gives in each case a quadratic equation in β . Thus, the extreme values of ν_{-} and ν_{+} are at $\beta = \beta_{-\pm}$ and $\beta = \beta_{+\pm}$, the roots of the quadratic equations. The first identity, (B 3)₁ was found by Ting & Chen (2005), their eqn (4.15).

To summarize the analysis for the three edges: extreme values of Poisson's ratio on the three edges are at the ends of edge 1, and on edges 2 and 3 given by ν_{+} of equations (B 2) and (B 3).

(a) Numerical proof of tables 1 and 2

A numerical test was performed over the range of possible materials. This required searching the entire two-dimensional range for α , β . Consideration of all possible materials then follows by allowing the material point to range throughout the triangle of figure 3. In every case, it is found that the extreme values of ν occur on the edge of the irreducible 1/48th element of the cube surface. Furthermore, the extreme values are never found to occur along edge 2. Extreme values on edge 3 in figure 2 can be found by considering edge 3' instead, i.e. $\alpha = 0$, $-1/6 < \beta < 0$. This implies as possible extrema one of $\nu_{-}(0, \beta_{-\pm})$ and one of $\nu_{+}(0, \beta_{+\pm})$. We define these as $\nu'_1 = \nu_{-}(0, \beta_{--})$ and $\nu'_2 = \nu_{+}(0, \beta_{+-})$, where the signs correspond to the sign of the discriminant in the roots, then they are given explicitly as

$$\nu_1' = \frac{-1}{2\left(1 - \frac{\chi_0}{3}\right)} \left\{ \left(\frac{\chi_0}{6} - \nu_0\right) + \left[\left(\frac{\chi_0}{6} - \nu_0\right)^2 + \frac{\chi_0}{12} \left(1 - \frac{\chi_0}{3}\right) \right]^{1/2} \right\},\tag{B 4}$$

$$\nu_2' = \frac{1}{2\left(1 - \frac{\chi_0}{3}\right)} \left\{ \left(1 + \nu_0 - \frac{\chi_0}{2}\right) + \left[\left(1 - \nu_0 - \frac{\chi_0}{6}\right)^2 + \frac{\chi_0}{12}\left(1 - \frac{\chi_0}{3}\right)\right]^{1/2} \right\}. \tag{B 5}$$

It may be checked that $\nu'_1 = \nu_1$ and $\nu'_2 = \nu_2$, in agreement with equation (3.19).

The numerical results indicate the potential extrema come from the five values: ν_0 , ν_{001} , $\nu_{1\bar{1}0}$, ν_1 and ν_2 . It turns out that each is an extreme for some range of material properties. Thus, the first four are necessary to define the global minimum, cf. table 1 and figure 4, while all five occur in the description of the global maximum, in table 2 and figure 5.

Although a mathematical proof has not been provided for the veracity of tables 1 and 2, and figures 4 and 5, it is relatively simple to do a numerical test, a posteriori. By performing the numerical search as described above, and

subtracting the extreme values of tables 1 and 2, one finds zero, or its numerical approximant for all points in the interior of the triangle of possible materials, figure 2.

In order to further justify the results as presented, appendix Bb gives arguments for the occurrence of the special values -1/2 and 3/2 in figures 4 and 5.

(b) Significance of
$$-1/2$$
 and $3/2$

Suppose Poisson's ratio is the same for two different pairs of directions: $\nu(n, m) = \nu(n^*, m^*)$. The pairs (n, m) and (n^*, m^*) must satisfy, using (4.2),

$$\frac{D(\boldsymbol{n}, \boldsymbol{m}) - D(\boldsymbol{n}^*, \boldsymbol{m}^*)}{F(\boldsymbol{n}) - F(\boldsymbol{n}^*)} = 2\nu.$$
(B 6)

For instance, let $\mathbf{n}^* = 110$, $\mathbf{m}^* = 001$, so that $\mathbf{v} = \mathbf{v}_{001}$. Equation (B 6) implies that the same Poisson's ratio is achieved for directions (\mathbf{n}, \mathbf{m}) satisfying

$$\frac{D(n,m)}{2F(n)-1/2} = \nu_{001}.$$
 (B 7)

Note that this is independent of ν_0 and χ_0 . We choose ν_{001} specifically because it has been viewed as the candidate for largest Poisson's ratio, until Ting & Chen (2005). If it is *not* the largest, then there must be pairs (n, m) other than (110,001) for which (B 7) holds. However, it may be shown using results from §2 that the minimum of the left member in (B 7) is 3/2, and the minimum occurs at n = 110, as one might expect. This indicates that ν_{001} must exceed 3/2 in order for the largest Poisson's ratio to occur for n other than the face diagonal 110.

Returning to (B 6), let $\nu = \nu_{1\bar{1}0}$, then $\nu(\boldsymbol{n}, \boldsymbol{m}) = \nu_{1\bar{1}0}$ if

$$\frac{\frac{1}{2} - D(\mathbf{n}, \mathbf{m})}{2F(\mathbf{n}) - \frac{1}{2}} = -\nu_{1\bar{1}0}.$$
 (B 8)

Using equation (2.8) and the previous result, it can be shown that the minimum of the left member in (B 8) is 1/2, and the minimum is at n = 110. Hence, $\nu_{1\bar{1}0}$ must be less than -1/2 in order for the smallest Poisson's ratio to occur for n other than the face diagonal 110. These two results explain why the particular values $\nu_{001} = 3/2$ and $\nu_{1\bar{1}0} = -1/2$ appear in tables 1 and 2 and in figures 4 and 5.

References

Baughman, R. H., Shacklette, J. M., Zakhidov, A. A. & Stafstrom, S. 1998 Negative Poisson's ratios as a common feature of cubic metals. *Nature* **392**, 362–365. (doi:10.1038/32842)

Boulanger, Ph. & Hayes, M. A. 1998 Poisson's ratio for orthorhombic materials. J. Elasticity 50, 87–89. (doi:10.1023/A:1007468812050)

Cazzani, A. & Rovati, M. 2003 Extrema of Young's modulus for cubic and transversely isotropic solids. Int. J. Solids Struct. 40, 1713–1744. (doi:10.1016/S0020-7683(02)00668-6)

Gunton, D. J. & Saunders, G. A. 1975 Stability limits on the Poisson ratio: application to a martensitic transformation. *Proc. R. Soc.* **343**, 68–83.

Hayes, M. A. 1972 Connexions between the moduli for anisotropic elastic materials. *J. Elasticity* $\bf 2$, 135-141. (doi:10.1007/BF00046063)

- Hayes, M. A. & Shuvalov, A. 1998 On the extreme values of Young's modulus, the shear modulus, and Poisson's ratio for cubic materials. J. Appl. Mech. ASME 65, 786–787.
- He, Q. C. 2004 Characterization of the anisotropic materials capable of exhibiting an isotropic Young or shear or area modulus. *Int. J. Eng. Sci.* 42, 2107–2118. (doi:10.1016/j.ijengsci.2004.04.009)
- Landolt, H. H. & Bornstein, R. 1992 Numerical data and functional relationships in science and technology, III/29/a. Second and higher order elastic constants. Berlin: Springer.
- Lempriere, B. M. 1968 Poisson's ratio in orthotropic materials. AIAA J. 6, 2226–2227.
- Love, A. E. H. 1944 Treatise on the mathematical theory of elasticity. New York, NY: Dover.
- Milstein, F. & Huang, K. 1979 Existence of a negative Poisson ratio in fcc crystals. *Phys. Rev. B* 19, 2030–2033. (doi:10.1103/PhysRevB.19.2030)
- Musgrave, M. J. P. 2003 Crystal acoustics. New York, NY: Acoustical Society of America.
- Norris, A. N. Submitted. Extreme values of Poisson's ratio and other engineering moduli in anisotropic solids.
- Scott, N. H. 2000 An area modulus of elasticity: definition and properties. J. Elasticity 58, 269–275. (doi:10.1023/A:1007675928019)
- Sirotin, Yu. I. & Shaskol'skaya, M. P. 1982 Fundamentals of crystal physics. Moscow: MIR.
- Thomson, W. 1856 Elements of a mathematical theory of elasticity. *Phil. Trans. R. Soc.* 146, 481–498.
- Ting, T. C. T. 2004 Very large Poisson's ratio with a bounded transverse strain in anisotropic elastic materials. *J. Elasticity* 77, 163–176. (doi:10.1007/s10659-005-2156-6)
- Ting, T. C. T. & Barnett, D. M. 2005 Negative Poisson's ratios in anisotropic linear elastic media. J. Appl. Mech. ASME 72, 929–931. (doi:10.1115/1.2042483)
- Ting, T. C. T. & Chen, T. 2005 Poisson's ratio for anisotropic elastic materials can have no bounds. Q. J. Mech. Appl. Math. 58, 73–82. (doi:10.1093/qjmamj/hbh021)
- Walpole, L. J. 1984 Fourth rank tensors of the thirty-two crystal classes: multiplication tables. *Proc. R. Soc.* A391, 149–179.
- Walpole, L. J. 1986 The elastic shear moduli of a cubic crystal. J. Phys. D: Appl. Phys. 19, 457–462. (doi:10.1088/0022-3727/19/3/014)